

# Influence of Fibre Arrangement on the Buckling Load of Composite Plates - Analytical Solution

DOI: 10.5604/12303666.1161764

Department of Strength of Material,  
Lodz University of Technology,  
Stefanowskiego 1/15, 90-924 Lodz, Poland  
E-mail: pawel\_czapski@interia.pl;  
tomasz.kubiak@p.lodz.pl

## Abstract

This paper deals with the problem of the influence of the angular arrangement of laminas on the buckling force of rectangular composite plates. The article presents a general, simple analytical method of buckling load determination and finding the best arrangement in terms of the highest stiffness in the prebuckling state. Some special characteristic cases of arrangements in an eight layered GFRP laminate are assumed, and buckling force as a function of the arrangement is investigated by finding proper maxima. Results for some characteristic lay-ups are compared with FEM and results found in literature.

**Key words:** laminate, fibred composites, analytical methods, plate theory, FEM analysis.

## Introduction

Composites are currently one of the most important classes of materials used in almost all branches of industry. A wide group of composite structures is represented by fiber reinforced polymers [3, 4], Fibred Metal Laminates or Sandwich Panels. They can be met in civil engineering (reinforcing windows or doors) [2], dentistry [10], orthopedics (implants) [7, 10], the automotive industry (housings and panels) [1], the aircraft industry (skins of airplanes, wings) [13, 17] or wind turbines (shovels) [9]. Their main advantage is a high strength to weight ratio. Instead of using pure metals or their alloys, which are usually very heavy, composites are used. This paper focuses

on fiber reinforced laminates and tries to theoretically answer the question how to arrange the angular orientation of each ply in a symmetric lay-up in order to increase the resistance to buckling. Similar theoretical considerations were already performed [12, 19]. However, the approach to the problem presented by previous authors is slightly different. Methods applied in the literature quoted are based on checking many lay-ups using iteration methods - many different combinations are compared or buckling load functions estimated. The method presented in this article differs from other approaches in its simplicity and investigation of whole critical force functions vs. the angle - not just special cases. Other publications also

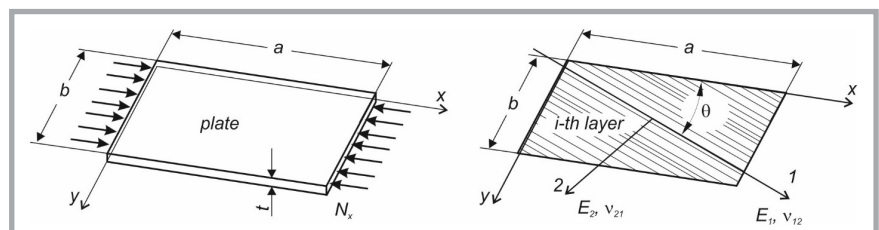


Figure 1. Plate with dimensions considered and coordinate system assumed.

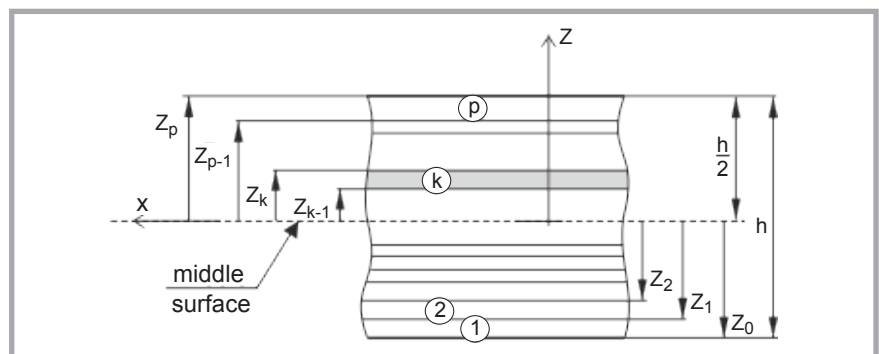


Figure 2. Numbering of plies.

include experimental and numerical [19] comparisons of results. Laminates are usually modelled as orthotropic materials. In order to consider all phenomena occurring in the laminates [11, 14] new elements for the Finite Element Method has been designed [6, 15, 18]. The Finite Element Method is a very powerful way to perform any type of strength analysis when analytical-numerical solutions usually have to contain simplifications. In the case of non-symmetric lay-ups of the laminas, analytical methods become more complicated and another numerical or analytical-numerical method should rather be applied [20] due to the appearance of non-zero values in elements of stiffness matrix **B**. These elements are responsible for unexpected phenomena e.g. twisting during compression or bending.

The main aim of this study was to prepare a simple analytical model that allows to find a function describing the influence of the angular arrangement of fibers with respect to midplane symmetric laminates on the buckling load. In order to show only analytic methods of determining the stiffest angular arrangements, the symmetry of the lay-up in an eight layered laminate is considered. A simple form of an analytical method has got some limitations – only the function of two variables can be investigated, which means that in the case of an arbitrary number of layers, the maximal value of variables introduced (in this case - angles can be two). The simplicity of the method presented may turn out to be very useful and quick during the design process of composite panels. Having just simple mathematical software (Mathematica or Matlab) or own software code optimisation, the problem of finding the highest stiffness of composite panels [17] can be easily solved.

## ■ Analytical solution

The method proposed is derived for rectangular composite plates with dimensions  $a \times b \times t$ , where  $a$  is a length of the plate,  $b$  – the width of the plate, and  $t$  is the plate thickness (*Figure 1*).

It was assumed that the plate is made of an 8 layer laminate with homogenized orthotropic material properties at each ply and symmetrical ply arrangement. However, by using the way of thinking presented, the number of layers can be decreased or increased. Knowing

$$\begin{aligned} \bar{Q}_{11} &= Q_{11} \cos^4 \theta + 2(Q_{12} + 2Q_{66}) \sin^2 \theta \cos^2 \theta + Q_{22} \sin^4 \theta, \\ \bar{Q}_{12} &= (Q_{11} + Q_{22} - 4Q_{66}) \sin^2 \theta \cos^2 \theta + Q_{12} (\sin^4 \theta + \cos^4 \theta), \\ \bar{Q}_{22} &= Q_{11} \sin^4 \theta + 2(Q_{12} + 2Q_{66}) \sin^2 \theta \cos^2 \theta + Q_{22} \cos^4 \theta, \\ \bar{Q}_{16} &= (Q_{11} - Q_{12} - 2Q_{66}) \sin \theta \cos^3 \theta + (Q_{12} - Q_{22} + 2Q_{66}) \sin^3 \theta \cos \theta, \\ \bar{Q}_{26} &= (Q_{11} - Q_{12} - 2Q_{66}) \sin^3 \theta \cos \theta + (Q_{12} - Q_{22} + 2Q_{66}) \sin \theta \cos^3 \theta, \\ \bar{Q}_{66} &= (Q_{11} + Q_{22} - 2Q_{12} - 2Q_{66}) \sin^2 \theta \cos^2 \theta + Q_{66} (\sin^4 \theta + \cos^4 \theta). \end{aligned} \quad (2)$$

$$\bar{N}_x = \pi^2 \left[ D_{11} \left( \frac{m}{a} \right)^2 + 2(D_{12} + 2D_{66}) \left( \frac{n}{b} \right)^2 + D_{22} \left( \frac{n}{b} \right)^4 \left( \frac{a}{m} \right)^2 \right] \quad (3)$$

$$D_{ij} = \frac{1}{3} \sum_{k=1}^N (\bar{Q}_{ij})_k (z_k^3 - z_{k-1}^3) = \sum_{k=1}^N (\bar{Q}_{ij})_k \left( \frac{t_k^3}{12} + \bar{t}z_k^2 \right) \quad (4)$$

$$\begin{aligned} D_{ij} &= \sum_{k=1}^N (\bar{Q}_{ij})_k \left( \frac{t_k^3}{12} + \bar{t}z_k^2 \right) = 2 \sum_{n=1}^n (\bar{Q}_{ij})_n \left( \frac{t_n^3}{12} + t \left( \frac{1}{2} (2n-1)t \right)^2 \right) = \\ &= \frac{2t^3}{3} \sum_{n=1}^n (\bar{Q}_{ij})_n (3n^2 - 3n + 1) = \\ &= \frac{2t^3}{3} (\bar{Q}_{ij})_1 + 7(\bar{Q}_{ij})_2 + 19(\bar{Q}_{ij})_3 + 37(\bar{Q}_{ij})_4 + \dots \end{aligned} \quad (5)$$

### Equations 2, 3, 4 and 5.

the Young modulus in two perpendicular directions  $E_1$  and  $E_2$ , Kirchhoff modulus  $G_{12}$  and Poisson ratio  $\nu_{12}$ , elements of the stiffness matrix for each ply can be calculated using well-known formulas [16]:

$$\begin{aligned} Q_{11} &= \frac{E_1}{1 - \nu_{12}\nu_{21}}, \\ Q_{22} &= \frac{E_2}{1 - \nu_{12}\nu_{21}}, \\ Q_{12} &= \frac{\nu_{12}E_2}{1 - \nu_{12}\nu_{21}}, \\ Q_{66} &= G_{12}, \end{aligned} \quad (1)$$

where  $\nu_{21}$ , according to the Betty-Maxwell theorem, can be calculated from:

$$\nu_{21} = \frac{E_2}{E_1} \nu_{12}.$$

The arrangement of the principle axes of orthotropy (fibres) can be rotated with some angle with respect to the main coordinate system, and the new  $Q$  coefficients of the stiffness matrix is expressed by [16] see *Equation 2*.

As has been mentioned, at the beginning the plate is assumed to be symmetric with respect to the midplane and even has a number of plies. Thus only the elements of matrix  $D$  (part of the stiffness matrix corresponding to bending) are needed to calculate the buckling load.

According to Jones [16], the buckling force of a composite plate simply supported on each edge and subjected to unidirectional compression, is equal to *Equation 3* where  $m$  and  $n$  are the numbers of halfwaves in the  $x$  and  $y$  directions (*Figure 1*), respectively, and then coefficients  $D_{ij}$ , for any case, are given by [16] see *Equation 4* where is the thickness of the  $k^{th}$  ply, and  $z_k$  is the distance from the geometric midplane to the middle of the  $k^{th}$  ply. For a symmetric arrangement of the plies with respect to the midplane, for even numbers of plies ( $k = 2n$ ) and plies with all the same thickness  $t$  (arrangement and , the following formula is valid see *Equation 5*.

At this stage of the considerations, a conclusion can be drawn that layers which are the most distant from the geometrical midplane of the plate have the greatest influence on coefficients  $D$ . In further considerations only the case of an 8 ply symmetric laminate with an angular arrangement equal to:  $[\theta_4, \theta_3, \theta_2, \theta_1, \theta_1, \theta_2, \theta_3, \theta_4]$  will be taken into account. In this case coefficients are equal to *Equation 6* (see page 94).

Introducing at most only two variables  $\alpha$  and  $\beta$  (denoting angle of ply orientations) the three cases of the angular arrangement of the plies have been consid-

$$\begin{aligned}
D_{11} &= \frac{2t^3}{3} (Q_{11} (\cos^4 \theta_1 + 7 \cos^4 \theta_2 + 19 \cos^4 \theta_3 + 37 \cos^4 \theta_4) + \\
&+ 2(Q_{12} + 2Q_{66}) (\sin^2 \theta_1 \cos^2 \theta_1 + 7 \sin^2 \theta_2 \cos^2 \theta_2 + 19 \sin^2 \theta_3 \cos^2 \theta_3 + 37 \sin^2 \theta_4 \cos^2 \theta_4) + \\
&+ Q_{22} (\sin^4 \theta_1 + 7 \sin^4 \theta_2 + 19 \sin^4 \theta_3 + 37 \sin^4 \theta_4)), \\
D_{12} &= \frac{2t^3}{3} ((Q_{11} + Q_{22} - 4Q_{66}) (\sin^2 \theta_1 \cos^2 \theta_1 + 7 \sin^2 \theta_2 \cos^2 \theta_2 + 19 \sin^2 \theta_3 \cos^2 \theta_3 + 37 \sin^2 \theta_4 \cos^2 \theta_4) + \\
&+ Q_{12} (\sin^4 \theta_1 + \cos^4 \theta_1) + 7(\sin^4 \theta_2 + \cos^4 \theta_2) + 19(\sin^4 \theta_3 + \cos^4 \theta_3) + 37(\sin^4 \theta_4 + \cos^4 \theta_4)), \\
D_{22} &= \frac{2t^3}{3} (Q_{11} (\sin^4 \theta_1 + 7 \sin^4 \theta_2 + 19 \sin^4 \theta_3 + 37 \sin^4 \theta_4) + \\
&+ 2(Q_{12} + 2Q_{66}) (\sin^2 \theta_1 \cos^2 \theta_1 + 7 \sin^2 \theta_2 \cos^2 \theta_2 + 19 \sin^2 \theta_3 \cos^2 \theta_3 + 37 \sin^2 \theta_4 \cos^2 \theta_4) + \\
&+ Q_{22} (\cos^4 \theta_1 + 7 \cos^4 \theta_2 + 19 \cos^4 \theta_3 + 37 \cos^4 \theta_4)), \\
D_{66} &= \frac{2t^3}{3} ((Q_{11} + Q_{22} - 2Q_{12} - 2Q_{66}) (\sin^2 \theta_1 \cos^2 \theta_1 + 7 \sin^2 \theta_2 \cos^2 \theta_2 + 19 \sin^2 \theta_3 \cos^2 \theta_3 + 37 \sin^2 \theta_4 \cos^2 \theta_4) + \\
&+ Q_{66} (\sin^4 \theta_1 + \cos^4 \theta_1) + 7(\sin^4 \theta_2 + \cos^4 \theta_2) + 19(\sin^4 \theta_3 + \cos^4 \theta_3) + 37(\sin^4 \theta_4 + \cos^4 \theta_4)).
\end{aligned} \tag{6}$$

$$\begin{aligned}
\sin(-x) &= -\sin x \text{ so } \sin^2(-x) = \sin^2 x \text{ and} \\
\cos(-x) &= \cos x \text{ so } \cos^2(-x) = \cos^2 x.
\end{aligned} \tag{7}$$

$$\begin{aligned}
D_{11} &= \frac{128}{3} t^3 (Q_{11} \cos^4 \alpha + 2(Q_{12} + 2Q_{66}) \sin^2 \alpha \cos^2 \alpha + Q_{22} \sin^4 \alpha), \\
D_{12} &= \frac{128}{3} t^3 ((Q_{11} + Q_{22} - 4Q_{66}) \sin^2 \alpha \cos^2 \alpha + Q_{12} (\sin^4 \alpha + \cos^4 \alpha)), \\
D_{22} &= \frac{128}{3} t^3 (Q_{11} \sin^4 \alpha + 2(Q_{12} + 2Q_{66}) \sin^2 \alpha \cos^2 \alpha + Q_{22} \cos^4 \alpha), \\
D_{66} &= \frac{128}{3} t^3 ((Q_{11} + Q_{22} - 2Q_{12} - 2Q_{66}) \sin^2 \alpha \cos^2 \alpha + Q_{66} (\sin^4 \alpha + \cos^4 \alpha)).
\end{aligned} \tag{8}$$

$$\begin{aligned}
D_{11} &= \frac{128}{3} t^3 (Q_{11} (20 \cos^4 \alpha + 44 \sin^4 \alpha) + 128(Q_{12} + 2Q_{66}) \sin^2 \alpha \cos^2 \alpha + Q_{22} (20 \sin^4 \alpha + 44 \cos^4 \alpha)), \\
D_{12} &= \frac{128}{3} t^3 ((Q_{11} + Q_{22} - 4Q_{66}) \sin^2 \alpha \cos^2 \alpha + Q_{12} (\sin^4 \alpha + \cos^4 \alpha)), \\
D_{22} &= \frac{128}{3} t^3 (Q_{11} (44 \cos^4 \alpha + 20 \sin^4 \alpha) + 128(Q_{12} + 2Q_{66}) \sin^2 \alpha \cos^2 \alpha + Q_{22} (44 \sin^4 \alpha + 20 \cos^4 \alpha)), \\
D_{66} &= \frac{128}{3} t^3 ((Q_{11} + Q_{22} - 2Q_{12} - 2Q_{66}) \sin^2 \alpha \cos^2 \alpha + Q_{66} (\sin^4 \alpha + \cos^4 \alpha)).
\end{aligned} \tag{10}$$

$$\begin{aligned}
D_{11} &= \frac{2}{3} t^3 (Q_{11} (\cos^4 \beta + 7 \sin^4 \beta + 19 \cos^4 \alpha + 37 \sin^4 \alpha) + \\
&+ (Q_{12} + 2Q_{66}) (8 \sin^2 \beta \cos^2 \beta + 56 \sin^2 \alpha \cos^2 \alpha) + Q_{22} (\sin^4 \beta + 7 \cos^4 \beta + 19 \sin^4 \alpha + 37 \cos^4 \alpha)), \\
D_{12} &= \frac{2}{3} t^3 ((Q_{11} + Q_{22} - 4Q_{66}) (8 \sin^2 \beta \cos^2 \beta + 56 \sin^2 \alpha \cos^2 \alpha) + \\
&+ Q_{12} (8(\sin^4 \beta + \cos^4 \beta) + 56(\sin^4 \alpha + \cos^4 \alpha))), \\
D_{22} &= \frac{2}{3} t^3 (Q_{11} (\sin^4 \beta + 7 \cos^4 \beta + 19 \sin^4 \alpha + 37 \cos^4 \alpha) + \\
&+ (Q_{12} + 2Q_{66}) (8 \sin^2 \beta \cos^2 \beta + 56 \sin^2 \alpha \cos^2 \alpha) + Q_{22} (\cos^4 \beta + 7 \sin^4 \beta + 19 \cos^4 \alpha + 37 \sin^4 \alpha)), \\
D_{66} &= \frac{2}{3} t^3 ((Q_{11} + Q_{22} - 2Q_{12} - 2Q_{66}) (8 \sin^2 \beta \cos^2 \beta + 56 \sin^2 \alpha \cos^2 \alpha) + \\
&+ Q_{66} (8(\sin^4 \beta + \cos^4 \beta) + 56(\sin^4 \alpha + \cos^4 \alpha))).
\end{aligned} \tag{11}$$

Equations 6, 7, 8, 10 and 11.

ered to verify and check the tendency for the buckling load in the midplane symmetric laminates. They are as follow:

case 1:  $[\alpha, -\alpha, \alpha, -\alpha, -\alpha, \alpha, -\alpha, \alpha]$ ,

case 2:  $[90^\circ + \alpha, \alpha, 90^\circ + \alpha, \alpha, \alpha, 90^\circ + \alpha, \alpha, 90^\circ + \alpha]$ ,

case 3:  $[90^\circ + \alpha, \alpha, 90^\circ + \beta, \beta, \beta, 90^\circ + \beta, \alpha, 90^\circ + \alpha]$ ,

where,  $\alpha$  and  $\beta$  angles can be change from  $-90^\circ$  to  $+90^\circ$ . The cases of layer ar-

rangements assumed allow to describe almost all types of midplane symmetric laminates in which the bending – stretching coupling as well as bending – twisting coupling are zero (deformation caused by the load are analogous to the structure of isotropic materials). It should be noted that midplane symmetric laminates are one of the most popular angular arrangements appearing in the literature [5, 20] and used in real structures.

In the first case  $[\alpha, -\alpha, \alpha, -\alpha, -\alpha, \alpha, -\alpha, \alpha]$ , the following two trigonometric identities have been used to solve this problem (Equation 7).

Then the  $D_{ij}$  coefficients are (see Equation 8).

The critical force is only a function of  $\alpha$ .

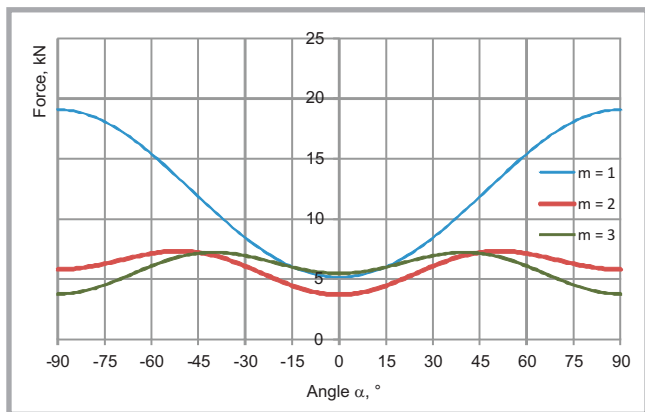


Figure 3. Plot force vs. angle for plate  $a = b = 100$  mm for arrangement.

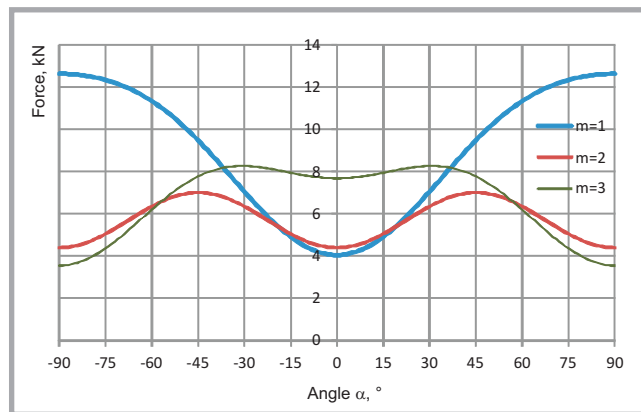


Figure 4. Plot force vs. angle for plate  $a = 2b = 200$  mm for arrangement.

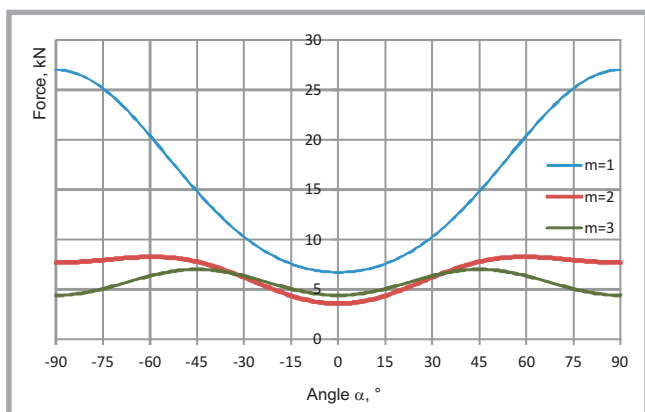


Figure 5. Plot force vs. angle for plate  $a = 3b = 300$  mm for arrangement.

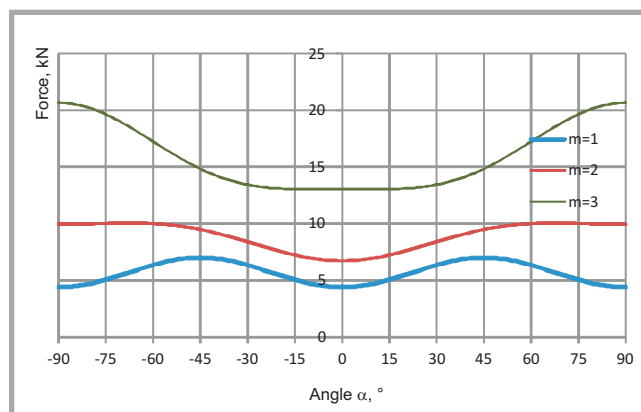


Figure 6. Plot force vs. angle for plate  $a = b = 100$  mm for arrangement.

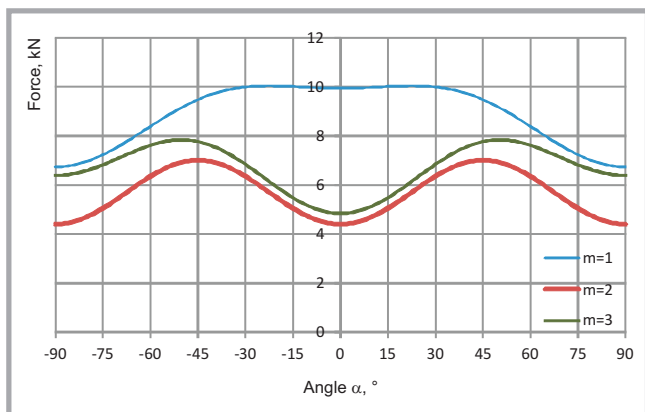


Figure 7. Plot force vs. angle for plate  $a = 2b = 200$  mm for arrangement.

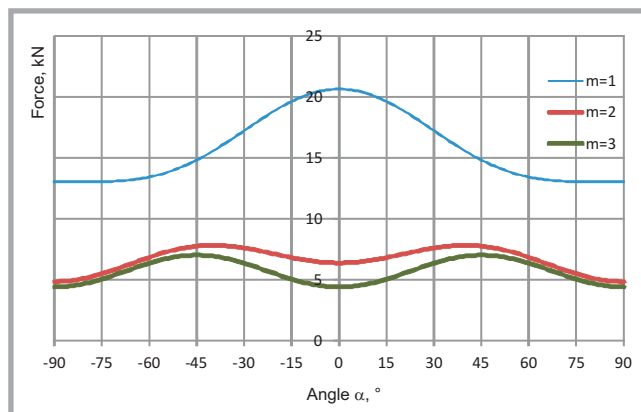


Figure 8. Plot force vs. angle for plate  $a = 3b = 300$  mm for arrangement.

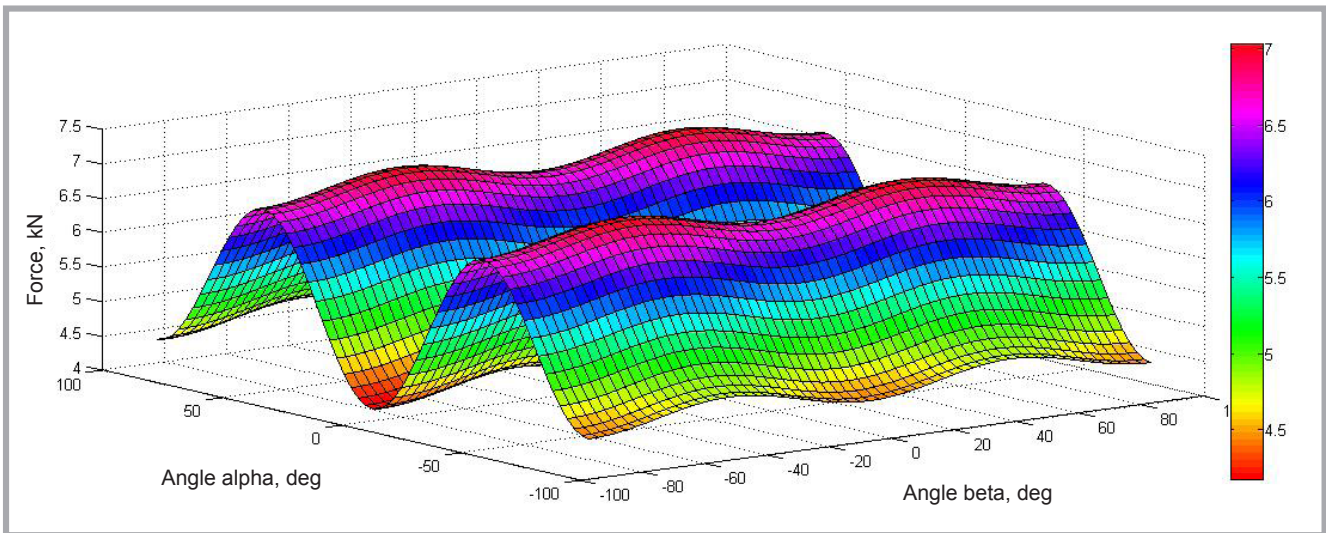


Figure 9. Plot force vs. angle for plate  $a = b = 100$  mm for arrangement: with buckling mode  $m = 1$ .

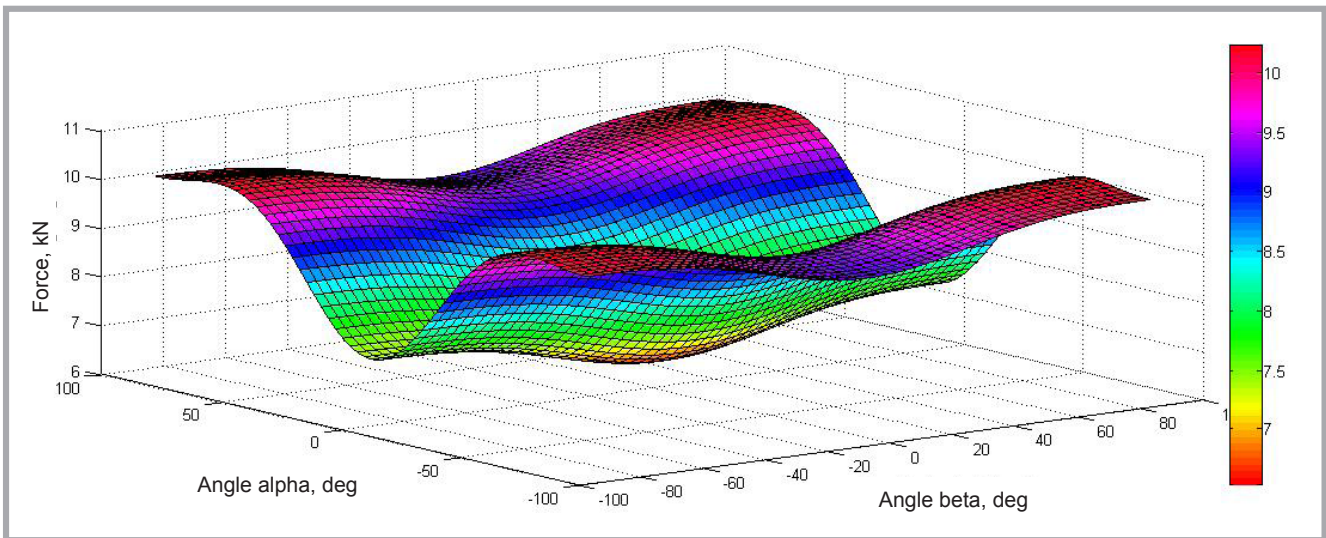


Figure 10. Force vs. angle for plate  $a = b = 100$  mm for arrangement: with buckling mode  $m = 2$ .

In the second case  $[90^\circ + \alpha, \alpha, 90^\circ + \alpha, \alpha, \alpha, 90^\circ + \alpha, \alpha, 90^\circ + \alpha]$  similar trigonometric identities have been used:

$$\begin{aligned} \sin(90^\circ + x) &= \cos x & \text{so} \\ \sin^2(90^\circ + x) &= \cos^2 x & \text{and} \\ \cos(90^\circ + x) &= -\sin x & \text{so} \\ \cos^2(90^\circ + x) &= \cos^2 x. \end{aligned} \quad (9)$$

Now the formulas for coefficients can be reduced to see **Equation 10** (see page 94).

To find the best arrangement in the third case  $[90^\circ + \alpha, \alpha, 90^\circ + \beta, \beta, \beta, 90^\circ + \beta, \alpha, 90^\circ + \alpha]$ , a function of two variables has to be introduced and a graph of the function must be considered in a 3D space. Similar to previous cases, the elements  $D_{ij}$  are as **Equation 11** (see page 94).

Knowing the coefficient of the bending stiffness matrix  $[D]$ , it is easy to calculate the buckling force for a rectangular plate using **Equation 11**. The results of exemplary calculations are presented in the next section.

### Exemplary results of calculations

Calculations were performed on rectangular composite plates with dimensions  $a \times b \times t$  made from GFRP laminate. Material properties are taken from the results of experimental tests [4] and assumed to be as follow:

- Young modulus:  $E_1 = 38.5$  GPa;
- Young modulus  $E_2 = 8.2$  GPa;
- Kirchhoff modulus:  $G_{12} = 1.92$  GPa;
- Poisson ratio:  $\nu_{12} = 0.27$ .

Necessary parameters of the laminate are as follow:

$$\begin{aligned} \nu_{21} &= E_2/E_1 \nu_{12} = 0.057, \\ Q_{11} &= E_1/(1 - \nu_{12} \nu_{21}) = 39.1 \text{ GPa} \\ Q_{22} &= E_2/(1 - \nu_{12} \nu_{21}) = 8.23 \text{ GPa} \\ Q_{12} &= \nu_{12} E_2/(1 - \nu_{12} \nu_{21}) = 2.22 \text{ GPa} \\ Q_{66} &= G_{12} = 1.92 \text{ GPa} \end{aligned} \quad (12)$$

In further considerations, the value of the thickness of the lamina was assumed to be  $t_k = 0.26$  mm. A series of three dimensions of the plates  $a = b = 100$  mm,  $a = 2b = 200$  mm, and  $a = 3b = 300$  mm have been taken into the calculations. Due to the simple axial load, it is assumed that in the  $b$  direction only one halfwave can occur.

The plots presented in **Figures 3 - 8** show the dependence between the critical force and angle for three values of

**Table 1.** Comparison of buckling loads FEM vs. the analytical method for some special cases of angular arrangement.

Arrangement	Plate a = b = 100 mm			Plate a = 2b = 200 mm			Plate a = b = 100 mm		
	m	F <sub>an</sub> , kN	F <sub>FEM</sub> , kN	m	F <sub>an</sub> , kN	F <sub>FEM</sub> , kN	m	F <sub>an</sub> , kN	F <sub>FEM</sub> , kN
[-45/45/-45/45] <sub>s</sub>	1	7.01	6.41	2	7.01	6.46	3	7.01	6.47
[30, -30, 30, -30] <sub>s</sub>	1	6.35	5.91	2	6.35	5.97	2	6.19	5.89
[-30, 60, -30, 60] <sub>s</sub>	1	6.35	5.89	2	6.35	5.88	3	6.35	5.86
[0, 90, 0, 90] <sub>s</sub>	1	4.39	4.35	2	4.39	4.36	3	4.39	4.36
[90, 0, 90, 0] <sub>s</sub>	1	4.39	4.35	2	4.39	4.36	3	4.39	4.36
[90, 0, 45, -45] <sub>s</sub>	1	4.74	4.63	2	4.74	4.63	3	4.74	4.65
[45/-45, 0, 90] <sub>s</sub>	1	6.69	6.19	2	6.69	6.24	3	6.69	6.24
[45/-45, 90, 0] <sub>s</sub>	1	6.69	6.19	2	6.69	6.24	3	6.69	6.24

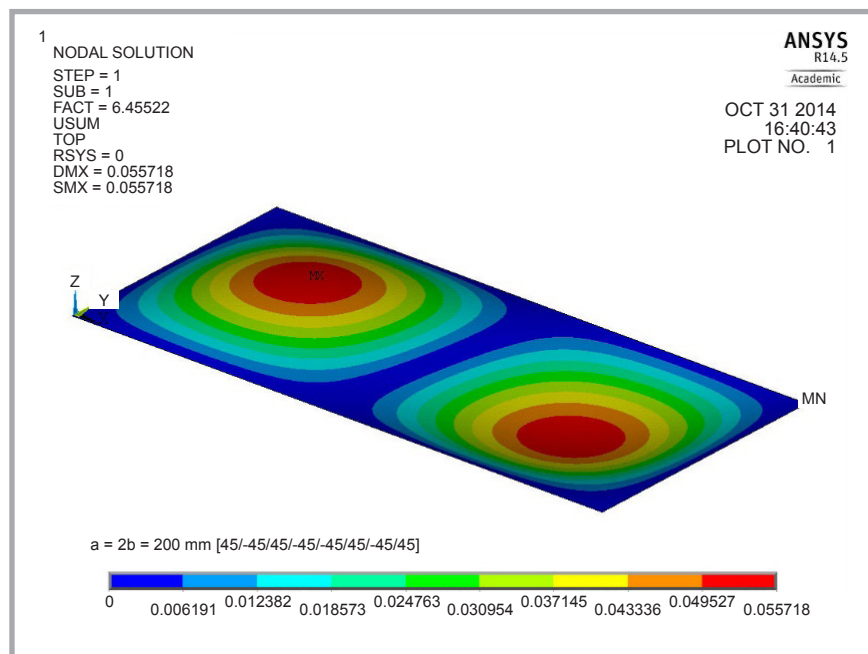


**Figure 11.** Exemplary FEM buckling mode for plate  $a = 2b = 200$  mm with arrangement [-45/45/-45/45].

half-waves in the longitudinal direction  $m = 1, 2$  &  $3$  for pairs  $a = b = 100$  mm,  $a = 2b = 200$  mm and  $a = 3b = 300$  mm. The buckling force should always be taken as the smallest one from curves corresponding to given buckling modes.

In the case of layer arrangements, 3D plots had to be prepared, and are presented in **Figures 9 – 10**.

In all of the cases of lay-ups assumed in terms of the variables, the highest stiffness is obtained by using arrangement [-45/45/-45/45/45/-45/45/-45] of layers. In plate  $a = 2b = 200$  mm even three buckling modes can occur depending on the angular orientation. Comparison of the analytical solution with FEM is presented in **Table 1**, and these results are in good agreement with numerical and experimental investigations. In [20] 12<sup>th</sup> layered symmetrical laminates were analysed using semi-analytical and finite

element methods. It turned out that the symmetrical arrangement which consists of only  $\pm 45$  plies still provides the highest buckling load even in higher number of plies. Experiments performed in [4, 5] showed that introducing a further 0/90 ply pairs decreases the critical force. Numerical predictions were in good agreement with experimental tests. According to the analysis performed, which includes only some special orthogonal pairs of arrangements, a conclusion can be drawn that lay-ups consisting of only  $\pm 45$  angles provides the highest buckling loads in all fibred materials, which are assumed to be ordered symmetrically with respect to the midplane. However, the experiments quoted showed that placing the two laminas near the midplane at 0 angles (e.g. [-45/45/-45/0/0/-45/45/-45]) can slightly increase the buckling load; however, according to assumed in this article, the sequences of plies cannot be proven.

**Table 1** presents minimal buckling forces with appropriate buckling mode  $m$  from FEM and the analytical solution for some specific arrangements. In all cases the buckling mode is the same for FEM and analytical results.

## Conclusions

The method presented gives results very comparable to FEM. The relative error turned out to be no higher than 2% in the case of arrangements including angles 0 and 90 and those not higher than 10% for lay-ups  $\pm 45^\circ$ . The results of experimental tests are proportional to those obtained from analytical, numerical and FEM methods. The main advantage of the way of calculations presented is its availability, simplicity and arbitrary number of plies which can be introduced. However, it also has disadvantages due to the limited number of variables introduced and validity only for symmetric lay-ups. According to calculations performed by other authors, a conclusion can be drawn that in the case of fibred laminates the highest buckling loads appear in arrangements composed of  $\pm 45^\circ$  plies. In the future, the method presented can be extended using other numerical methods, introducing an arbitrary number of variables.

Glass and carbon fibre laminates have a lot of advantages in terms of proper design. They provide a high strength to weight ratio and a very wide range of appropriate materials. After choosing proper material, forming of the composite can still be controlled by the designers by angular arrangements of the fibres, as presented in this paper.

The analytical method presented can be used in the form presented or extended for more layers and be used in the design process, which could be important in situations where a quick evaluation of construction stability is needed. Such a problem may occur when the mechanical system is too heavy, and due to this fact it does not fulfill its tasks - as a very good example the elements in aircraft can be quoted. Before standard FEM analysis of the whole plane it is good to evaluate the stiffness of some parts - this approach seems to be ideal for this purpose. In the future, the authors will verify experimentally tendencies presented for other structures, such as complicated shaped columns, not only simple plates.



## Acknowledgement

The paper has been written under a research project financed by the National Centre for Science - decision number DEC-2011/03/B/ST8/06447

## References

1. Bisagni Ch, Di Pietro G, Frascini L, Terletti D. Progressive Crushing of Fiber-Reinforced Composite Structural Components of a Formula one Racing Car. *Composite Structures* 2005; 68: 491–503.
2. Abid A. Shah, Ribakov Y. Recent trends in steel fibered high-strength concrete. *Materials and Design* 2011; 32: 4122–4151.
3. Dębski H. Experimental investigation of post-buckling behavior of composite column with top-hat cross-section. *Eksploatacja i Niezawodność – Maintenance and Reliability* 2013; 15(2): 106–110.
4. Dębski H, Kubiak T, Teter A. Experimental investigation of channel-section composite profiles behavior with various sequences of plies subjected to static compression. *Thin-Walled Structures* 2013; 71: 147–154.
5. Dębski H, Teter A, Kubiak T. Numerical and experimental studies of compressed composite columns with complex open cross-sections. *Composite Structures* 2014; 118: 28–36.
6. Barbero EJ, Madeo A, Zagari G, Zinno R, Zucco G. A mixed isostatic 24 dof element for static and buckling analysis of laminated folded plates. *Composite Structures* 2014; 116: 223–234.
7. Hassan Mehboob, Seung-Hwan Chang. Application of composites to orthopedic prostheses for effective bone healing: A review. *Composite Structures* 2014; 118: 328–341. doi:10.1016/j.compstruct.2014.07.052.
8. Bienias J, Gliszczynski A, Jakubczak P, Kubiak T, Majerski K. Influence of autoclaving process parameters on the buckling and postbuckling behaviour of thin-walled channel section beams. *Thin-Walled Structures* 2014; 85: 262–270.
9. Zangenberg J, Brøndsted P, Koefoed M. Design of a fibrous composite preform for wind turbine rotor blades. *Materials and Design* 2014; 56: 635–641.
10. Fujihara K, Teo K, Gopal R, Loh PL, Ganesh VK, Ramakrishna S, Foong KWC, Chew CL. Fibrous composite materials in dentistry and orthopaedics: review and applications. *Composites Science and Technology* 2004; 64: 775–788.
11. Kumar D, Singh SB. Effects of flexural boundary conditions on failure and stability of composite laminate with cutouts under combined in-plane loads. *Composites: Part B* 2013; 45: 657–665.
12. Avalle M, Belingardi G. A theoretical Approach to the optimization of flexural stiffness of symmetric laminates. *Composite structures* 1995; 31(1): 75–86.
13. Mangalgiri PD. Composite materials for aerospace applications. *BullMaterSci* 1999; 22(3): 657–64.
14. Heidari-Rarani M, Khalkhali-Sharifi SS, Shokrieh MM. Effect of ply stacking sequence on buckling behavior of E-glass/ epoxy laminated composites. *Computational Materials Science* 2014; 89: 89–96.
15. Nam-Il Kim 1, Dong-Ho Choi. Super convergent shear deformable finite elements for stability analysis of composite beams. *Composites: Part B* 2013; 44: 100–111.
16. Jones RM. *Mechanics of composite materials*. Ed. London: Taylor & Francis, 1999.
17. Rośkowicz M, Smal T. Research on durability of composite materials used in repairing aircraft components. *Eksploatacja i Niezawodność. Maintenance and Reliability* 2013; 15(4): 349–355.
18. Ghannadpour SAM, Ovesy HR, Zia-Dehkordi E. An exact finite strip for the calculation of initial post-buckling stiffness of shear deformable composite laminated plates. *Composite Structures* 2014; 108: 504–513.
19. Wei Wang, Guo S, Nan Chang, Wei Yang. Optimum buckling design of composite stiffened panels using ant colony algorithm. *Composite Structures* 2010; 92: 712–719.
20. Kołakowski Z, Mania RJ. Semi-analytical method versus the FEM for analysis of the local post-buckling of thin-walled composite structures. *Composite Structures* 2013; 97: 99–106.

Received 06.11.2014 Reviewed 22.03.2015



## INSTITUTE OF BIOPOLYMERS AND CHEMICAL FIBRES LABORATORY OF METROLOGY

**Contact:** Beata Pałys M.Sc. Eng.  
ul. M. Skłodowskiej-Curie 19/27, 90-570 Łódź, Poland  
tel. (+48 42) 638 03 41, e-mail: metrologia@ibwch.lodz.pl



AB 388

The **Laboratory** is active in testing fibres, yarns, textiles and medical products. The usability and physico-mechanical properties of textiles and medical products are tested in accordance with European EN, International ISO and Polish PN standards.

### Tests within the accreditation procedure:

- linear density of fibres and yarns, ■ mass per unit area using small samples, ■ elasticity of yarns, ■ breaking force and elongation of fibres, yarns and medical products, ■ loop tenacity of fibres and yarns, ■ bending length and specific flexural rigidity of textile and medical products

### Other tests:

- **for fibres:** ■ diameter of fibres, ■ staple length and its distribution of fibres, ■ linear shrinkage of fibres, ■ elasticity and initial modulus of drawn fibres, ■ crimp index, ■ tenacity
- **for yarn:** ■ yarn twist, ■ contractility of multifilament yarns, ■ tenacity,
- **for textiles:** ■ mass per unit area using small samples, ■ thickness
- **for films:** ■ thickness-mechanical scanning method, ■ mechanical properties under static tension
- **for medical products:** ■ determination of the compressive strength of skull bones, ■ determination of breaking strength and elongation at break, ■ suture retention strength of medical products, ■ perforation strength and dislocation at perforation

### The Laboratory of Metrology carries out analyses for:

- research and development work, ■ consultancy and expertise

### Main equipment:

- Instron tensile testing machines, ■ electrical capacitance tester for the determination of linear density unevenness - Uster type C, ■ lanameter